

Original Article

# Distribution and expression of Pen-2 in the central nervous system of APP/PS1 double transgenic mice

Yanan Chu<sup>1,†</sup>, Xuehua Peng<sup>2,†</sup>, Zhiming Long<sup>3</sup>, Kejian Wang<sup>3</sup>, Shifang Luo<sup>3</sup>, Akhilesh Sharma<sup>1</sup>, and Guiqiong He<sup>1,3,\*</sup>

<sup>1</sup>Institute of Neuroscience, Chongqing Medical University, Chongqing 400016, China, <sup>2</sup>Department of Radiology, Pediatric Hospital, Chongqing Medical University, Chongqing 400016, China, and <sup>3</sup>Department of Anatomy, Chongqing Medical University, Chongqing 400016, China

<sup>†</sup>These authors contributed equally to this work.

\*Correspondence address. Tel: +86-23-68485763; Fax: +86-23-68485000; E-mail: guiqionghe@hotmail.com

Received 10 November 2014; Accepted 22 December 2014

## Abstract

The  $\gamma$ -secretase complex catalyzes the final cleavage step of amyloid  $\beta$ -protein precursor (APP) to generate amyloid  $\beta$  (A $\beta$ ) peptide, a pathogenic component of senile plaques in the brain of Alzheimer's disease (AD) patients. Recent studies have shown that presenilin enhancer-2 (Pen-2), presenilin (PS, including PS1 and PS2), nicastrin, and anterior pharynx-defective 1 are essential components of the  $\gamma$ -secretase. The structure and function of Pen-2 *in vitro* have been well defined. However, little is known about the neuroanatomical distribution and expression of Pen-2 in the central nervous system (CNS) of AD model mice. We report here, using various methods such as immunohistochemical staining and immunoblotting, that Pen-2 is widely expressed at specific neuronal cells of major areas in AD model mice, including the olfactory bulb, basal forebrain, striatum, cortex, hippocampus, amygdala, thalamus, hypothalamus, cerebellum, brainstem, and spinal cord. It is co-expressed with PS1 in specific neuronal cells in mouse brain. Pen-2 is distributed much more extensively than extracellular amyloid deposits, suggesting the importance of other factors in localized amyloid deposition. Pen-2 is localized predominantly in cell membrane and cytoplasm in adult AD mice, but only distributed at cell membrane in controls. At the early stages of postnatal development, the expression level of Pen-2 is relatively high in CNS, but declines, gradually in adult mice. The present study provides an anatomical basis for Pen-2 as a key component of  $\gamma$ -secretase complex in the brain of developing and adult mice, and Pen-2 might be closely related to A $\beta$  burden in aging nervous system.

**Key words:** presenilin enhancer-2,  $\gamma$ -secretase, Alzheimer's disease, central nervous system, distribution

## Introduction

Alzheimer's disease (AD) is the most common cause of dementia and the most prevalent neurodegenerative disorder. It is featured by progressive impairment of memory and deterioration of comprehensive cognition [1]. Senile neuritic plaque (SP) is the pathological hallmark

lesion in the brains of AD patients. Amyloid  $\beta$  (A $\beta$ ) peptide was first identified as the aggregated protein deposited within the core of SP [2]. A $\beta$  monomer may be harmless [3]; however, it can self-assemble into A $\beta$  oligomers, larger A $\beta$  aggregation intermediates, and eventually the fibrillar aggregates that notoriously deposit in the brains of AD

patients [4]. A $\beta$  is produced from successive cleavages of the type I transmembrane glycoprotein amyloid  $\beta$ -protein precursor (APP) by  $\beta$ - and  $\gamma$ -secretase [5].  $\gamma$ -Secretase cleaves APP within its transmembrane domain, yielding mainly 40- and 42-amino acid A $\beta$  C-terminal variants, A $\beta$ 40 and A $\beta$ 42 [6]. According to the ‘amyloid cascade hypothesis’, the ratio of A $\beta$ 42/A $\beta$ 40 might be a key factor in the development and pathogenesis of AD [7]. Thus,  $\gamma$ -secretase becomes an attractive drug target for AD. Besides APP,  $\gamma$ -secretase also cleaves many other substrates, most notably the Notch receptor, the cleavage product of which is required for signaling essential to all metazoans [8].

Genetic and biochemical researches suggest that  $\gamma$ -secretase is a high-molecular-weight multi-protein complex, which contains at least four subunits: presenilin (PS, including PS1 and PS2), nicastrin (Nct), anterior pharynx-defective 1 (Aph-1), and PS enhancer-2 (Pen-2). These four components have been shown to be essential and sufficient for  $\gamma$ -secretase activity [9]. PS, the best studied component of the  $\gamma$ -secretase complex, forms functional PS NTF/CTF heterodimer that acts as the catalytic core of  $\gamma$ -secretase complex [10]. Nct is initially identified as a binding partner of PS and is needed to stabilize PS expression [11]. It is also thought to be responsible for substrate recruitment because of its large extracellular domain [12]. Aph-1 and Nct assemble into a stable subcomplex, which then interacts with the CTF of PS [13,14]. The smallest subunit Pen-2 is a small hairpin-like membrane protein, and it is initially identified in *Caenorhabditis elegans* via genetic screening for modifiers of the PS homologs [15]. Pen-2 facilitates the autocatalytic cleavage of PS, producing two fragments known as the CTF and NTF. Over-expression of Pen-2 induces an elevation in  $\gamma$ -secretase activity and subsequent A $\beta$ 42 production. The down-regulation of Pen-2 may lead to deficient  $\gamma$ -secretase complex formation, reduction of PS level [16,17], and PS endoproteolysis [18–20]. Recent studies have revealed that Pen-2 is more than a structural component of the  $\gamma$ -secretase complex [21] and may play a key role in the regulation of  $\gamma$ -secretase activity [22].  $\gamma$ -Secretase modulator that reduces A $\beta$ 42 generation binds mainly to Pen-2 [23]. Furthermore, a novel coding mutation (S73F) of Pen-2 was identified in a woman from an Italian family with AD [24]. Sequence variations of Pen-2 may also increase the risk for sporadic AD cases [25], making Pen-2 a reasonable AD-related gene. A recent study shows that over-expression of Pen-2 in NSE/hPen-2 transgenic mice may play an important role in the development of pathological features of AD and A $\beta$ 42 deposition [26]. These studies clearly establish that Pen-2 is a key regulator of  $\gamma$ -secretase and modulator of A $\beta$  production.

However, few researches have been reported on the neuroanatomical distribution and expression of Pen-2 either in the adult or in the developing mammalian central nervous system (CNS). In this study, we attempted to characterize the location of Pen-2 in mice brain and spinal cord, and its expression during the postnatal developmental stages in mice. Results showed that Pen-2 distributes extensively in all major brain areas and spinal cord, and it is co-localized with PS1. Pen-2 immunoreactivity is associated with plaques, but distributes much more widely than extracellular amyloid deposits. In addition, Pen-2 expression level exhibits a declined tendency during postnatal development in mouse brain. Furthermore, our study also showed that Pen-2 expression is relatively higher in brain of AD model mice than that of the controls. Our results not only provide an anatomical basis for the function of Pen-2 as an essential component of  $\gamma$ -secretase complex in the developing and adult mouse brain, but also indicate that Pen-2 might be closely related to A $\beta$  burden in aging nervous system.

## Materials and Methods

### Animals

APP/PS1 double transgenic mice (APP<sup>swe</sup>, PSEN1 $\Delta$ 9) (Jackson Lab, Bar Harbor, USA) carried the mouse/human APP695cDNA with the Swedish mutation and mutant human PS1 (PS1- $\Delta$ 9). The genotype of the mice was confirmed by PCR using DNA from tail tissues. The wild-type littermates were used as normal controls. Adult male mice (25–35 g) and postnatal mice from different developmental stages, i.e. postnatal day 1 (P1), P7, and P21 were housed and maintained in accordance with guidelines approved by the Animal Protection and Ethics Committee of Chongqing Medical University (Chongqing, China).

### Tissue preparation

The experiment conformed to the international guidelines on ethical use of animals, and minimized the number of animals used and their suffering. Animal handling and tissue harvesting were carried out as described by Gao *et al.* [27]. Eight adult APP/PS1 mice and control mice (4-month old) were anesthetized with 2% chloral hydrate and sacrificed by decapitation. In parallel, four mice from each of the following postnatal developmental stages, i.e. P1, P7, and P21 were decapitated. The brain was divided into two halves. One half was immediately homogenized for protein and the other half was postfixed with freshly prepared 4% paraformaldehyde (PFA) in 0.1 M phosphate-buffered saline (PBS, pH 7.4) for 8 h. All procedures were performed on ice. PFA-fixed brain tissues were dehydrated in graded ethanol and embedded in paraffin, then cut into 10  $\mu$ m-thick sagittal or coronal sections using a paraffin slicing machine (Leica Microsystems, Wetzlar, Germany). Sections were mounted onto slides for immunohistochemical (IHC) and immunofluorescent (IF) stainings.

### IHC and IF stainings

The slices were deparaffinized and then incubated in 0.3% Triton X-100 and 3% H<sub>2</sub>O<sub>2</sub> in PBS for 30 min, washed, and blocked with PBS containing 5% milk and 0.1% Triton X-100 for 1 h. Sections were then immunostained with rabbit anti-Pen-2 polyclonal antibody (1:200; Abcam Inc., Cambridge, USA) or mouse monoclonal 4G8 antibody (1:500; Convance Inc., Princeton, USA). Control staining was performed by omission of primary antibody. Incubation in primary antibody was conducted overnight at 4°C in Tris-buffered saline (TBS) supplemented with 3% normal goat serum and 0.05% Triton X-100. After being washed in PBS, sections were incubated with biotinylated goat anti-rabbit IgG antibody (1:200; Vector Laboratories, Burlingame, USA) for 1 h at room temperature followed by avidin–biotin–peroxidase complex (ABC, 1:100; Vector Laboratories). The reaction product was visualized with diaminobenzidine in the presence of H<sub>2</sub>O<sub>2</sub>. The micrographs of immunostaining were captured by a microscope (Leica Microsystems) equipped with a digital camera.

Confocal immunofluorescent microscopy was used to examine the co-localization of Pen-2 and PS1. Slide-mounted sections were incubated overnight at 4°C with rabbit anti-Pen-2 (1:200) and mouse anti-PS1 polyclonal antibody (1:1000; Bioss, Woburn, USA) in TBS containing 3% normal goat serum and 0.05% Triton X-100. Secondary antibodies were anti-rabbit Alexa-488 and anti-mouse Alexa-568 (at 1:800 each; Molecular Probes, Eugene, USA) prepared in the same buffer as the primary antibodies. Labeled tissues were examined with a laser scanning confocal microscope (Zeiss, Oberkochen, Germany)

and images were captured and digitized from individual 0.5  $\mu\text{m}$  optical sections. Background fluorescence was evaluated by omission of one or the other primary antibody.

### Cell counting and image analysis

Light micrographs were analyzed with aid of Image-Pro Plus 6.0 Analysis System (Media Cybernetics Inc., San Francisco, USA). The total number of Pen-2<sup>+</sup> cells in 10  $\mu\text{m}$  hemisection was counted using a microscopic field at a magnification of 400 $\times$ . Five sections per mouse were averaged to provide a single value for each mouse. The percentage of positive cells identified by intensely stained cell bodies was assessed. In addition, the mean integrated optical density (MIOD = IOD/total area) was measured to assess immunostaining level of Pen-2 in each region.

### Western blot analysis

Brain areas (such as cortex, septum, striatum, hippocampus, thalamus, cerebellum, brainstem, and spinal cord) were dissected and homogenized in RIPA lysis buffer (PIERCE, Rockford, USA). In parallel, four mice brains from embryonic stage (E17) and postnatal developmental stages (P1, P7, P21, and P120) were lysed in Tris lysis buffer. Supernatant was collected after centrifugation at 14,000 g for 15 min at 4°C. The protein concentration in the supernatant was determined by a protein assay kit (Bio-Rad, Hercules, USA). Equal amounts of protein (50  $\mu\text{g}$ ) were resolved by a 4%–16% Tris-tricine sodium dodecyl sulfate–polyacrylamide gel electrophoresis (SDS-PAGE) (Sigma-Aldrich, Mississauga, Canada). The proteins were then transferred onto polyvinylidene fluoride membranes (Millipore, Billerica, USA). Rabbit anti-Pen-2 polyclonal antibody (1:1000; Abcam Inc.) was used for detection. Internal control  $\beta$ -actin was analyzed using mouse monoclonal anti- $\beta$ -actin antibody (1:3000; Santa Cruz Biotechnology Inc., Santa Cruz, USA). Peroxidase-conjugated anti-rabbit IgG antibodies were used as secondary antibodies (1:50,000; Jackson Immuno-research Laboratories, West Grove, USA) and incubated for 1 h. Immunoreactive bands were visualized by enhanced chemiluminescent detection kit (Amersham Pharmacia Biotech, Buckinghamshire, UK) by exposure to X-ray film (Fuji Medical X-ray film) and then quantitated by Quantity one Analysis (Bio-Rad).

### Statistical analysis

All data were analyzed using SPSS statistics package. Data were presented as the mean  $\pm$  SEM. Statistical comparisons were made using an analysis of variance followed by a Student's *t*-test. *P* values <0.05 were considered statistically significant.

## Results

### Expression of Pen-2 protein in mice CNS

Since the expression of Pen-2 in the CNS has been rarely examined, we first did western blot analysis to examine the localization and expression of Pen-2 in the adult mice brain and spinal cord. Results showed that the Pen-2 antiserum identified one band with apparent molecular weight of 11 kDa (Fig. 1A). The Pen-2 protein was expressed in all major areas of the adult mice CNS, including the cortex, hippocampus, septum, striatum, thalamus, cerebellum, brainstem, and spinal cord.

Previous studies revealed that PS1-immunoreactive cells were distributed throughout the brain [11,28]. To determine whether Pen-2 and PS1 are co-localized in the adult mice brain, double IF staining

was carried out. As shown in Fig. 1B, Pen-2 existed in PS1-positive neurons in brain regions, such as cerebral cortex, hippocampus, and cerebellum.

### Pen-2 immunoreactivity in mice brain and spinal cord

We then examined the localization of Pen-2 in the CNS. Results showed that Pen-2-positive cells were found throughout the CNS of both adult AD model mice and its wild-type controls, including the olfactory bulb, basal forebrain, cerebral cortex, hippocampus, amygdala, thalamus, hypothalamus, cerebellum, brainstem, and spinal cord. Importantly, region-specific and neuron-specific differences were found in Pen-2 immunoreactivity, which was evident mainly in neurons and fibers but not in glial cells.

### Distribution profile of Pen-2 immunoreactivity seen in specific brain regions of APP/PS1 mice

#### Olfactory bulb

Numerous Pen-2-positive cells were observed in various regions of the olfactory bulbs with varying degrees of staining intensity. A number of labeled neurons were observed in glomerular layer (GL), mitral cell layer (ML), and granule cell layer (GRL), and few Pen-2-positive neurons were found in olfactory nerve fiber layer (NFL), external plexiform layer (EPL), and internal plexiform layer (IPL). Pen-2-positive neurons were strongly labeled in ML and GL, but moderately stained in GRL (Fig. 2a).

#### Basal forebrain and basal ganglia

Pen-2-positive neurons were distributed in all subregions of the basal forebrain, including the septum, nucleus basalis of Meynert, and diagonal band complex. We observed several moderately labeled multipolar cells in septal nuclei, while some intensely stained neurons along with weakly stained neurons in the diagonal band complex. We also noticed a number of moderately stained neurons in the bed nucleus of the stria terminalis and nucleus basalis of Meynert, a group of small neurons in the globus pallidus, ventral pallidum, and entopeduncular nucleus, and a subset of Pen-2<sup>+</sup> cells scattered throughout the caudate putamen (Fig. 2b,c).

#### Cerebral cortex

In most layer of the neocortex, Pen-2-positive cells with varying degrees of staining intensity were identified. Characteristically, the labeling was high in layers II–VI and relatively low in layer I. The lamina distribution of Pen-2-positive neurons was more obvious in cingulate cortex and in the frontoparietal cortex than in other cortical areas. Generally speaking, a number of moderately labeled neurons intermingled with strongly stained neurons were observed in layers II and IV, while most of the pyramidal neurons located in layers III and V were intensely labeled with vertically oriented apical dendrites. Some moderate somatodendritic labeling was seen in layer VI of the cortex. In the piriform cortex, intensely labeled Pen-2-positive neurons were observed in both the pyramidal and polymorphic layers, along with a smaller group of weakly labeled neurons (Fig. 2d–f).

#### Hippocampus

Some of the most intense and abundant Pen-2 immunoreactivity was observed in the hippocampal formation. Specifically, intense staining was seen in the CA1–CA3 pyramidal cell layer located within the Ammon's horn. Actually, all pyramidal neurons and their apical dendrites, which were usually found projecting into the adjoining



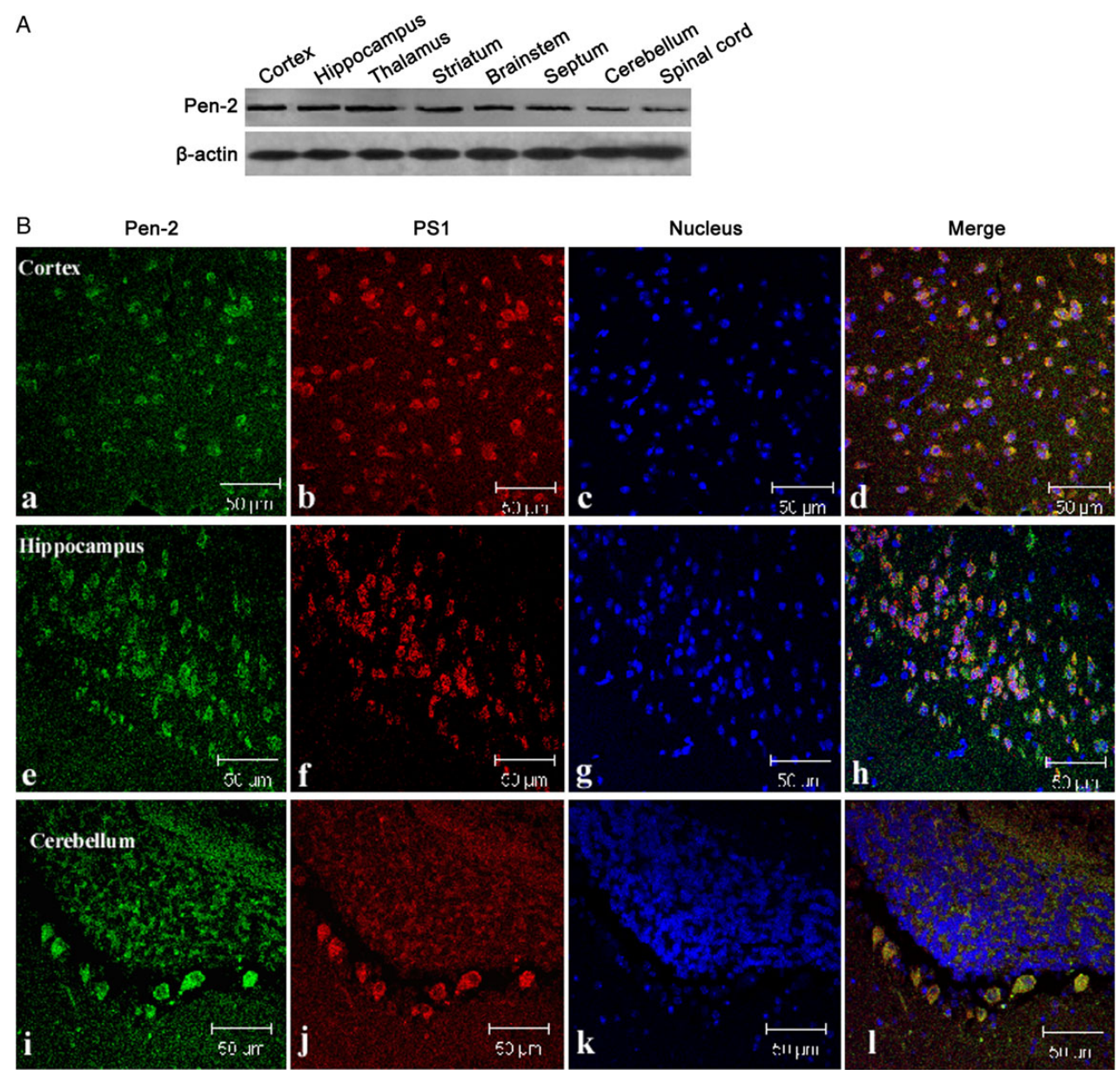


**Figure 1. Pen-2 expression in the mice CNS** (A) Western blot analysis of Pen-2 expression in spinal cord and different regions of the adult mice brain. The blot was re-probed with mouse anti-β-actin antibody as the loading control. Mouse brain and spinal cord were harvested at age of 4-month old. In total, 50 μg of proteins were separated on SDS-PAGE, western blotted, and probed with anti-Pen-2 and anti-β-actin antibodies, respectively. (B) Double IF staining analysis of Pen-2 and PS1 staining in adult mice cerebral cortex (a–d), hippocampus (e–h), and cerebellum (i–l). Scale bar = 50 μm.

stratum radiatum layer, exhibited strong labeling. Some multipolar neurons were scattered throughout the strata oriens and strata radiatum. Within the dentate gyrus, granule cell somata were strongly stained. Heavily stained neurons were also seen in the hilus region of hippocampus, whereas less Pen-2 immunoreactivity was observed in the adjacent molecular layer (Fig. 2g–i).

**Amygdala**

Several subsets of Pen-2-positive neurons with moderate staining were found in the cortical, medial, and basolateral amygdaloid nuclei. In the amygdaloid nuclei, Pen-2 immunoreactivity was found to be predominantly associated with cell bodies (Fig. 2j).

**Thalamus and hypothalamus**

A number of Pen-2-positive neurons were observed in the subregions of thalamus (Fig. 2k). In ventral and lateral portions of the thalamus and in the habenular nucleus, Pen-2-positive neurons were moderately stained. In the hypothalamus (Fig. 2l), a rather strong Pen-2 neuronal labeling was seen in the supraoptic and paraventricular nuclei, whereas neurons in the ventromedial nucleus, dorsolateral hypothalamic areas, and arcuate nucleus were rather weak or moderately immunostained.

**Brainstem**

Pen-2 immunoreactivity was seen at all levels of brainstem. A number of multipolar neurons with intense Pen-2 staining were observed in the



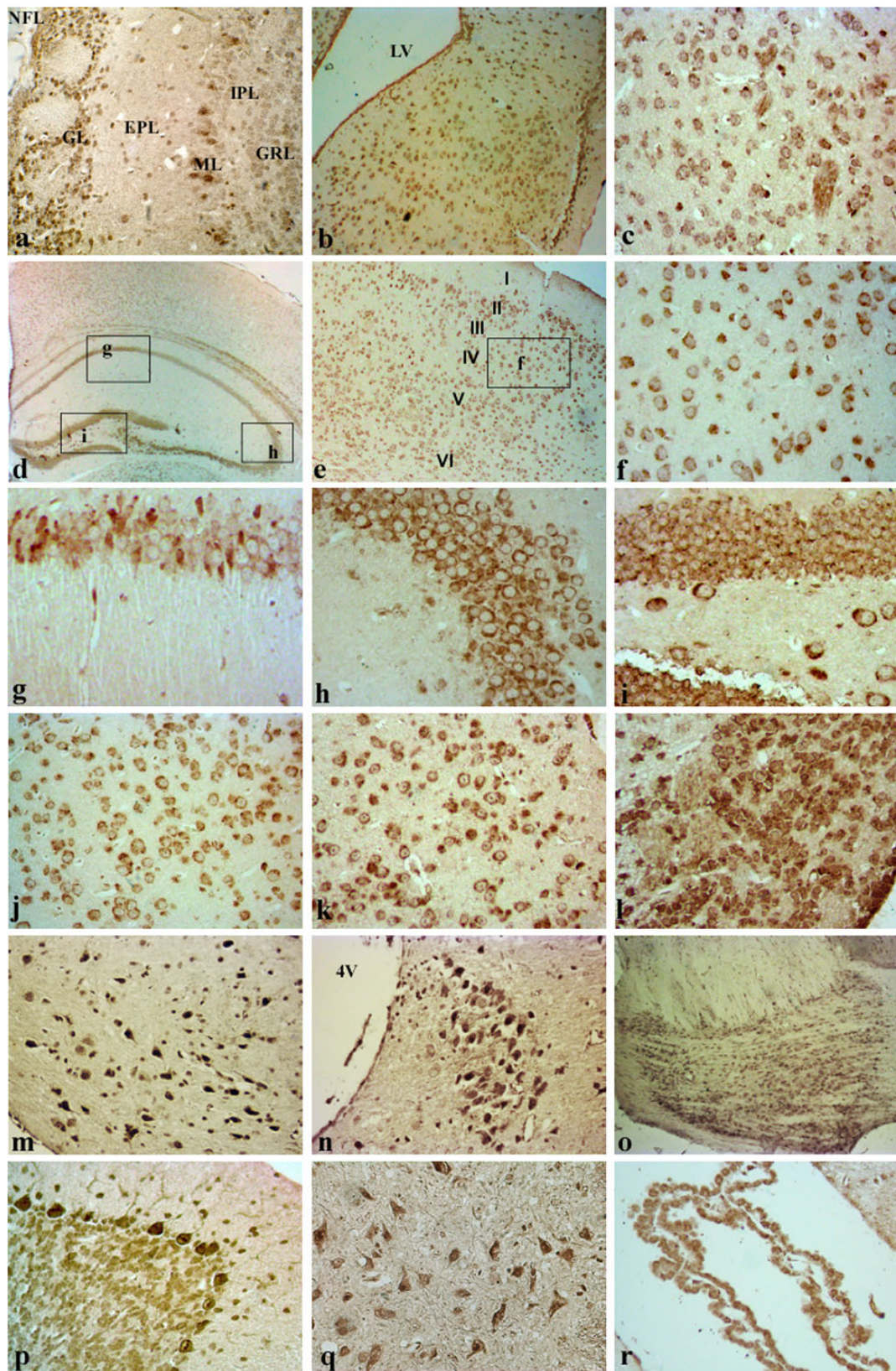


**Figure 2. Distribution of Pen-2 in the brain and spinal cord of APP/PS1 double transgenic mice** IHC staining showed the expression pattern of Pen-2 in the brain and spinal cord of APP/PS1 double transgenic mice: (a) olfactory bulb, (b) septal nuclei, (c) striatum, (d-f) cerebral cortex, (g-i) CA1, CA3, and dentate gyrus, (j) amygdala, (k) thalamus, (l) hypothalamus, (m) facial nucleus, (n) cochlear nucleus, (o) pontine nucleus, (p) cerebellum, (q) spinal cord, and (r) choroid plexus. a-c,  $\times 400$ ; d,  $\times 40$ ; e,  $\times 100$ ; f-r,  $\times 400$ . NFL, olfactory nerve fiber layer; GL, glomerular layer; EPL, external plexiform layer; ML, mitral cell layer; IPL, internal plexiform layer; GRL, granule cell layer; LV, lateral ventricle; 4V, 4th ventricle.



oculomotor nucleus, abducens nucleus, facial nucleus (Fig. 2m), motor trigeminal nucleus, and nucleus of solitary tract; and strong labeling was also evident in mesencephalic nucleus of trigeminal nerve, vestibular nucleus (Fig. 2n), pontine nucleus of trigeminal nerve (Fig. 2o), pontine reticular nucleus, locus ceruleus, and inferior olivary nucleus. However, the most intense labeling was seen especially in the oculomotor nucleus, facial nucleus, motor trigeminal nucleus, and vestibular nucleus. In addition, Pen-2-positive neurons with multipolar process were seen in the dorsal raphe nucleus, ventral and dorsal parts of the cochlear nucleus.

#### Cerebellum

Strong Pen-2 immunoreactivity was evident throughout the cerebellum. In the cortex, Purkinje cells were heavily labeled (Fig. 2p). The granule cells displayed rather weak staining, whereas numerous weak to moderate somatodendritic labeling occurred in the deep cerebellar nuclei.

#### Spinal cord

Pen-2-positive cells with varying degrees of staining intensity were observed throughout the full length of spinal cord. The most intense labeling was evident in the large neurons of ventral horn and a subset of medium or small size neurons in dorsal and lateral horns (Fig. 2q).

#### Choroid plexus

Strong immunoreactivity was observed in all epithelial cells on the surface of the choroid villi (Fig. 2r). There was no staining in the pial tissue or capillaries on the core of the villi.

#### Distribution of Pen-2 is related to amyloid deposits in the APP/PS1 transgenic mouse CNS

The APP/PS1 double transgenic mouse develops SP in an aging-dependent manner. To examine the relationship between A $\beta$  deposits

and Pen-2, we compared their locations in the CNS of 8-month-old APP/PS1 double transgenic mouse. IHC staining showed that a number of SPs with various sizes were observed in the cortex, hippocampus, and olfactory bulb, and fewer deposits were seen in the striatum, cerebellum, brainstem, and thalamus; while spinal cord was relatively devoid of A $\beta$  deposition at this stage. Pen-2-positive neurons were shown in amyloid-rich and amyloid-poor regions, and Pen-2 was expressed at similar levels in amyloid-rich and amyloid-poor regions. However, Pen-2 immunoreactivity was obviously intensified in some A $\beta$  deposits. At high magnification, Pen-2 immunoreactivity was increased throughout amyloid deposits (Fig. 3).

#### Comparison of Pen-2 expression in the brains of APP/PS1 and wild-type mice

We then compared the expression level of Pen-2 in the brains of adult AD model mice and wild-type controls. As shown in Fig. 4A, the distribution patterns of Pen-2<sup>+</sup> cells in brains of both groups were similar. However, the degree of Pen-2 staining intensity was different at cellular level between two groups. We observed that Pen-2 was localized predominantly in cell membrane and cytoplasm, and a number of heavily stained Pen-2<sup>+</sup> cells were visible in APP/PS1 mice, whereas in wild-type controls, Pen-2 was almost distributed near cell membrane and weakly labeled. The optical density of Pen-2<sup>+</sup> cells in AD model mice ( $1.55 \pm 0.21$ ) was much higher than that in wild-type mice ( $1.18 \pm 0.24$ ,  $t = 4.95$ ,  $P < 0.01$ , Fig. 4B). Western blot analysis also revealed an increase of Pen-2 expression in APP/PS1 mice when compared with controls (Fig. 4C,D).

#### Pen-2 immunoreactivity in the postnatal developing mice brain

Several studies have shown that  $\gamma$ -secretase subunit PS1 is expressed at relatively high level in embryonic brain, and then declined gradually

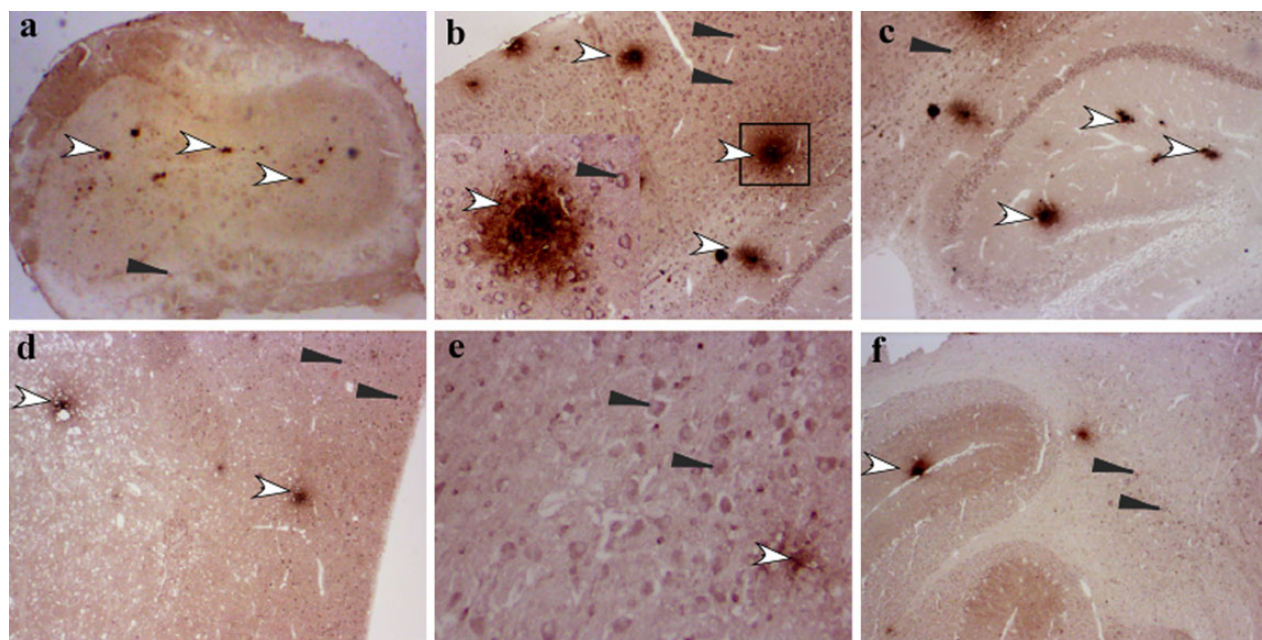


**Figure 3. Association of Pen-2 with SPs in the amyloid-bearing APP/PS1 mouse brain** Sections were shown from 8-month-old APP/PS1 double transgenic mouse brain labeled for SPs with mouse A $\beta$  antibody 4G8 and rabbit anti-Pen-2 antibody. IHC staining showed that a number of SPs with various sizes were seen in the olfactory bulb (a), hippocampus (b), and cortex (c), and fewer deposits were seen in the thalamus (d), brainstem (e), and cerebellum (f). Pen-2 is associated with plaques, but is expressed at similar levels in amyloid-rich and amyloid-poor regions. Inset in (b) showed Pen-2 labeling around SP at higher magnification. a–d and f:  $\times 100$ ; g:  $\times 400$ . White arrowheads point to SP and black arrowheads point to Pen-2<sup>+</sup> cells.

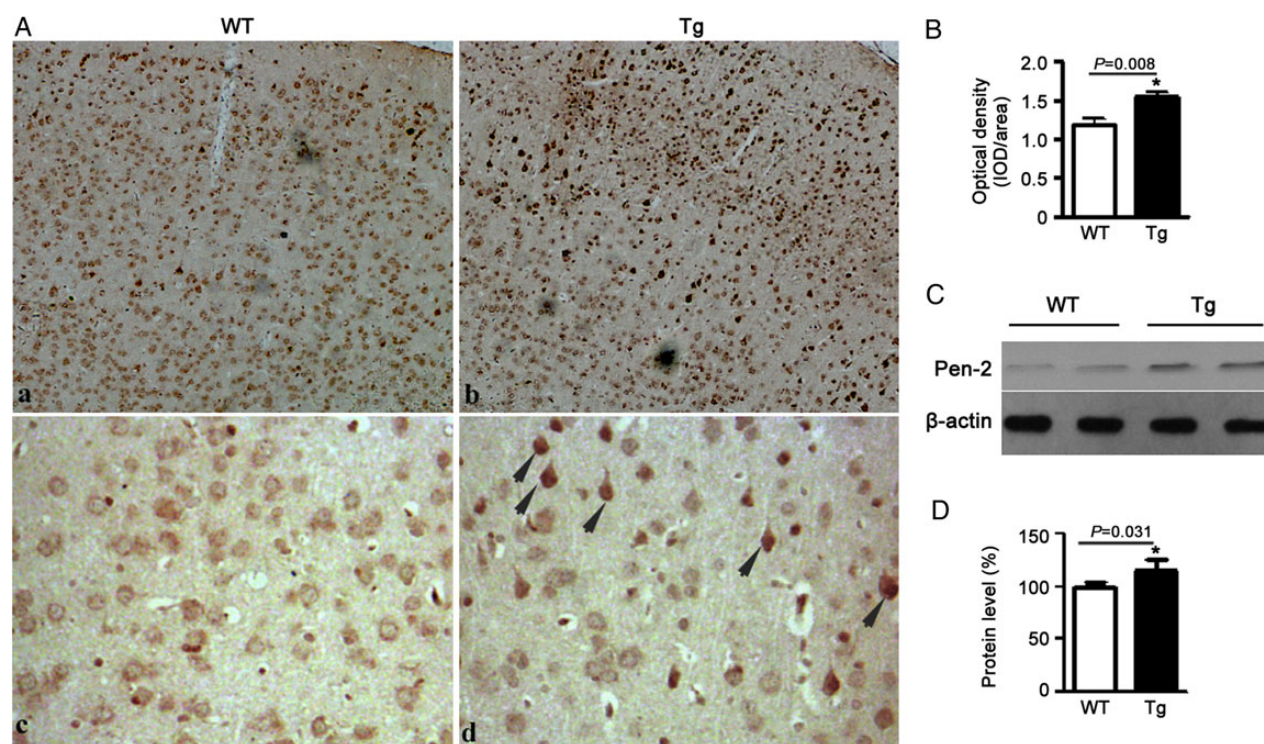


**Figure 4. Comparison of Pen-2 expression in the brains of APP/PS1 and wild-type mice** (A) IHC staining analysis showed the increased expression of Pen-2 in the cortex of adult APP/PS1 (Tg) mice when compared with wild-type (WT) controls. a and b:  $\times 100$ ; c and d:  $\times 400$ . Black arrowheads point to darkly stained Pen-2<sup>+</sup> cells. (B) Quantitative analysis of the optical density of Pen-2-positive neurons ( $n=9$ ,  $*P<0.05$  vs. control mice). (C) Western blot showed the expression of Pen-2 in APP/PS1 and control mice (two representatives were shown,  $n=4$ ). (D) Quantifications showed the significant elevation of Pen-2 expression in APP/PS1 mice compared with controls ( $*P<0.05$  vs. control mice).

during postnatal development of the brain [29,30]. To determine whether the distribution and expression level of Pen-2 are also developmentally regulated, IHC staining and western blotting were used to examine the Pen-2 expression in the cortex and hippocampus obtained from P1, P7, P21, and P120 brains. At cellular level (Fig. 5A), we observed that Pen-2 was expressed at all stages of the postnatal developing brains. The intensity of Pen-2 staining and the density of Pen-2<sup>+</sup> cells were high at early stage (i.e. P1), whereas at later stages (i.e. P21 and adult), the labeling intensity and the number of Pen-2<sup>+</sup> cells were found to be decreased gradually. Western blot analysis also revealed that high level of Pen-2 expression was found in embryonic mouse brain, but gradually declined to the lower adult level after birth (Fig. 5B,C).

## Discussion

$\gamma$ -Secretase cleaves APP to release A $\beta$  peptides that likely play a causative role in the pathogenesis of AD. In addition,  $\gamma$ -secretase cleaves Notch and other type I membrane proteins. Pen-2 is an essential cofactor of the  $\gamma$ -secretase complex, and its expression enhances the affinity or the accessibility of the substrate to the catalytic site of  $\gamma$ -secretase [31]. The abnormality of Pen-2 may accelerate AD pathology. Despite the physiological significance of Pen-2 function, knowledge is lacking on Pen-2 distribution in the CNS of APP/PS1 double transgenic AD model mice. The present study provides the first comprehensive cellular distribution profile of Pen-2 in the postnatal developing and adult mice CNS.

In this study, B6C3-Tg mice which carry mouse/human Swedish mutant APP 695 and human mutant PS1 transgene were used as AD model. B6C3-Tg mice begin to develop plaques at  $\sim 2.5$  months of age,

and behavioral impairments often precede brain A $\beta$  deposition [27,32]. At present, APP/PS1 transgenic mice are used by several laboratories for researches on the mechanisms of amyloid deposition as well as for the development of a therapy to prevent and/or cure AD.

Our immunoblotting data showed that Pen-2 is widely expressed in all major areas in mouse CNS. Double IF staining analysis revealed that Pen-2 distribution extensively coexisted with PS1 immunoreactivity in various regions of the adult mice brain, therefore, providing an anatomical basis for a physiological role for  $\gamma$ -secretase complex in a wide spectrum of neurons located throughout the brain.

However, IHC staining analysis revealed a clear variation in the staining intensity at different brain areas as well as labeling of individual cells. At cellular level, Pen-2-positive staining was apparent in neurons, but Pen-2 expression in astrocytes of AD mice brain cannot be excluded based on the present findings. Areas with relatively strong expression level of Pen-2 include the cerebral cortex, hippocampus, selected hypothalamic nuclei, Purkinje cells of the cerebellum, and motoneurons of brainstem. Some of these regions (such as cortex and hippocampus) are most vulnerable to pathological changes associated with AD.

A $\beta$  (especially A $\beta$ 42) is deposited into SP in a circumscribed manner in brain regions of human AD [33] as well as transgenic AD mouse models [34]. But the factors accounting for localized SP are largely unknown. Pen-2 is the last subunit incorporated into  $\gamma$ -secretase complex to trigger its activation and secretion of A $\beta$ . Recent study demonstrated that N-terminus of Pen-2 affects the structure of the active site of  $\gamma$ -secretase in a way to increase A $\beta$ 42 generation [35]. In the present study, we compared the spatial relationship between A $\beta$  deposits and Pen-2 expression in AD model mice. Intense deposition of amyloid occurs in the cerebral cortex, hippocampus, and olfactory bulb.



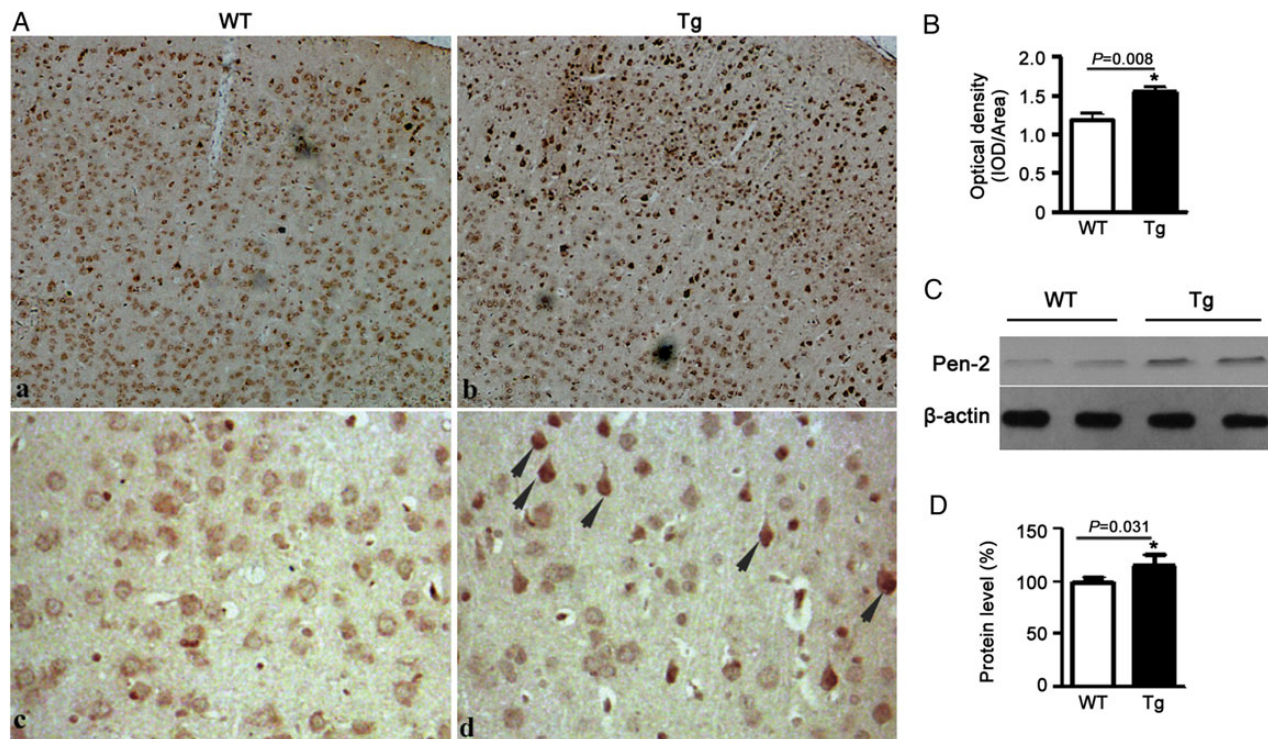


**Figure 5. Expression of Pen-2 during postnatal development** (A) IHC staining showed the expression pattern of Pen-2 in the cortex of the postnatal mice brains: (a) at postnatal day 1 (P1), (b) at P7, (c) at P21, and (d) at P120 (4 months). a–d:  $\times 100$ . (B) Immunoblot analysis of Pen-2 expression during postnatal brain development. Mouse brains were harvested at the indicated stages of embryonic and postnatal development. A total of 50  $\mu$ g proteins were separated by SDS-PAGE, analyzed by western blotting, and probed with anti-Pen-2 and anti- $\beta$ -actin antibodies, respectively. (C) Intensity of Pen-2 band was quantified from analysis of three animals and normalized to  $\beta$ -actin levels. High embryonic expression of Pen-2 gradually declined after birth. \* $P < 0.05$ , \*\* $P < 0.01$  vs. P1.

Meanwhile, we found that Pen-2 is expressed in both amyloid-rich brain regions (such as cortex and hippocampus) and amyloid-poor brain regions (such as cerebellum and spinal cord). This is somewhat consistent with a recent study which showed that local distribution of  $\gamma$ -secretase subunits or their levels of expression do not coincide with circumscribed amyloid deposition [36]. Interestingly, we noted that Pen-2 expression is relatively high in some amyloid deposits. In addition, we also found that Pen-2 expression is increased in APP/PS1 double mutant mouse brain. However, whether the increased Pen-2 expression in AD model mice is caused by its abnormal synthesis, abnormal degradation, or some other reasons is still unknown. Further study is needed to explore the underlying mechanism.

In addition to its role in A $\beta$  generation and AD,  $\gamma$ -secretase possesses different substrates such as Notch, E-cadherin, and ErbB-4 [37,38], which may play a key role in the development. Our studies reveal a pronounced postnatal developmental change of Pen-2 in AD model mouse brain. We found that Pen-2 protein level is relatively high during the early stages of embryonic development, and then declines in the course of postnatal development. Our data indicate that as a necessary component of  $\gamma$ -secretase complex, Pen-2 may also be involved in regulating neurogenesis and synaptogenesis during development.

In summary, the present study demonstrates clearly that Pen-2 is extensively distributed in the brain and spinal cord of adult APP/PS1 double transgenic AD model mice and its normal controls. Its expression level decreases during postnatal development in mouse brain. Pen-2 is distributed much more extensively than highly circumscribed SP, and Pen-2 expression is abundant in some deposits. Pen-2 expression is higher in brains of AD model mice than in wild-type controls. Further explorations are needed to determine

whether these characteristics of Pen-2 are signs of localized hotspots of  $\gamma$ -secretase activity or reflect a function of Pen-2 independent of the  $\gamma$ -secretase.

## Funding

This work was supported by the grants from the National Natural Science Foundation of China (Nos. 81371221 and 30700885) and the Program for New Century Excellent Talents in University (No. NCET-11-1084).

## References

- Mattson MP. Pathways towards and away from Alzheimer's disease. *Nature* 2004, 430: 631–639.
- Masters CL, Simms G, Weinman NA, Multhaup G, McDonald BL, Beyreuther K. Amyloid Plaque core protein in Alzheimer disease and down syndrome. *Proc Natl Acad Sci USA* 1985, 82: 4245–4249.
- Giuffrida ML, Caraci F, de Bona P, Pappalardo G, Nicoletti F, Rizzarelli E, Copani A. The monomer state of  $\beta$ -amyloid: where the Alzheimer's disease protein meets physiology. *Rev Neurosci* 2010, 21: 83–93.
- Kodali R, Wetzel R. Polymorphism in the intermediates and products of amyloid assembly. *Curr Opin Struct Biol* 2007, 17: 48–57.
- Tanzi RE, Bertram L. Twenty years of the Alzheimer's disease amyloid hypothesis: a genetic perspective. *Cell* 2005, 120: 545–555.
- Acx H, Chávez-Gutiérrez L, Serneels L, Lismont S, Benurwar M, Elad N, De Strooper B. Signature amyloid  $\beta$  profiles are produced by different  $\gamma$ -secretase complexes. *J Biol Chem* 2014, 289: 4346–4355.
- Xu X.  $\gamma$ -Secretase catalyzes sequential cleavages of the A $\beta$ PP transmembrane domain. *J Alzheimers Dis* 2009, 16: 211–224.



8. De Strooper B, Iwatsubo T, Wolfe MS. Presenilins and gamma-secretase: structure, function, and role in Alzheimer disease. *Cold Spring Harb Perspect Med* 2012, 2: a006304.
9. De Strooper B. Aph-1, Pen-2, and nicastrin with presenilin generate an active gamma-secretase complex. *Neuron* 2003, 38: 9–12.
10. Wolfe MS, Xia W, Ostaszewski BL, Diehl TS, Kimberly WT, Selkoe DJ. Two transmembrane aspartates in presenilin-1 required for presenilin endoproteolysis and gammasecretase activity. *Nature* 1999, 398: 513–517.
11. Edbauer D, Winkler E, Haass C, Steiner H. Presenilin and nicastrin regulate each other and determine amyloid beta-peptide production via complex formation. *Proc Natl Acad Sci USA* 2002, 99: 8666–8671.
12. Shah S, Lee SF, Tabuchi K, Hao YH, Yu C, LaPlant Q, Ball H, et al. Nicastrin functions as a gamma-secretase-substrate receptor. *Cell* 2005, 122: 435–447.
13. LaVoie M, Fraering PC, Ostaszewski BL, Ye W, Kimberly WT, Wolfe MS, Selkoe DJ. Assembly of the gamma-secretase complex involves early formation of an intermediate subcomplex of Aph-1 and nicastrin. *J Biol Chem* 2003, 278: 37213–37222.
14. Gu Y, Chen F, Sanjo N, Kawarai T, Hasegawa H, Duthie M, Li W, et al. APH-1 interacts with mature and immature forms of presenilins and nicastrin and may play a role in maturation of presenilin-nicastrin complexes. *J Biol Chem* 2003, 278: 7374–7380.
15. Steiner H, Winkler E, Edbauer D, Prokop S, Basset G, Yamasaki A, Kostka M, et al. PEN-2 is an integral component of the gamma-secretase complex required for coordinated expression of presenilin and nicastrin. *J Biol Chem* 2002, 277: 39062–39065.
16. Francis R, McGrath G, Zhang J, Ruddy DA, Sym M, Apfeld J, Nicoll M, et al. Aph-1 and pen-2 are required for Notch pathway signaling, gamma-secretase cleavage of  $\beta$ APP, and presenilin protein accumulation. *Dev Cell* 2002, 3: 85–97.
17. Prokop S, Shirotani K, Edbauer D, Haass C, Steiner H. Requirement of PEN-2 for stabilization of the presenilin N/C-terminal fragments heterodimer within the gamma-secretase complex. *J Biol Chem* 2004, 279: 23255–23261.
18. Kim SH, Ikeuchi T, Yu C, Sisodia SS. Regulated hyperaccumulation of presenilin-1 and the “gamma-secretase” complex. Evidence for differential intramembranous processing of transmembrane substrates. *J Biol Chem* 2003, 278: 33992–34002.
19. Takasugi N, Tomita T, Hayashi I, Tsuruoka M, Niimura M, Takahashi Y, Thinakaran G, et al. The role of presenilin cofactors in the gamma-secretase complex. *Nature* 2003, 422: 438–441.
20. Luo WJ, Wang H, Li H, Kim BS, Shah S, Lee HJ, Thinakaran G, et al. PEN-2 and APH-1 coordinately regulate proteolytic processing of presenilin 1. *J Biol Chem* 2003, 278: 7850–7854.
21. Holmes O, Paturi S, Selkoe DJ, Wolfe MS. Pen-2 is essential for  $\gamma$ -secretase complex stability and trafficking but partially dispensable for endoproteolysis. *Biochemistry* 2014, 53: 4393–4406.
22. Bammens L, Chávez-Gutiérrez L, Tolia A, Zwijsen A, De Strooper B. Functional and topological analysis of Pen-2, the fourth subunit of the gamma-secretase complex. *J Biol Chem* 2011, 286: 12271–12282.
23. Kounnas MZ, Danks AM, Cheng S, Tyree C, Ackerman E, Zhang X, Ahn K, et al. Modulation of  $\gamma$ -secretase reduces  $\beta$ -amyloid deposition in a transgenic mouse model of Alzheimer’s disease. *Neuron* 2010, 67: 769–780.
24. Albani D, Batelli S, Pesaresi M, Prato F, Polito L, Forloni G, Pantieri R. A novel PSENEN mutation in a patient with complaints of memory loss and a family history of dementia. *Alzheimers Dement* 2007, 3: 235–238.
25. Andreoli V, Trecroci F, La Russa A, Cittadella R, Liguori M, Spadafora P, Caracciolo M, et al. Presenilin enhancer-2 gene: identification of a novel promoter mutation in a patient with early-onset familial Alzheimer’s disease. *Alzheimers Dement* 2011, 7: 574–578.
26. Nam SH, Seo SJ, Goo JS, Kim JE, Choi SI, Lee HR, Hwang IS, et al. Pen-2 overexpression induces A $\beta$ 42 production, memory defect, motor activity enhancement and feeding behavior dysfunction in NSE/Pen-2 transgenic mice. *Int J Mol Med* 2011, 28: 961–971.
27. Gao B, Long Z, Zhao L, He G. Effect of normobaric hyperoxia on behavioral deficits and neuropathology in Alzheimer’s disease mouse model. *J Alzheimers Dis* 2011, 27: 317–326.
28. Blanchard V, Czech C, Bonici B, Clavel N, Gohin M, Dalet K, Revah F, et al. Immunohistochemical analysis of presenilin 2 expression in the mouse brain: distribution pattern and co-localization with presenilin 1 protein. *Brain Res* 1997, 758: 209–217.
29. Wines-Samuelson M, Shen J. Presenilins in the developing, adult, and aging cerebral cortex. *Neuroscientist* 2005, 11: 441–451.
30. Uchihara T, Sanjo N, Nakamura A, Han K, Song SY, St George-Hyslop P, Fraser PE. Transient abundance of presenilin 1 fragments/nicastrin complex associated with synaptogenesis during development in rat cerebellum. *Neurobiol Aging* 2006, 27: 88–97.
31. Shiraishi H, Sai X, Wang HQ, Maeda Y, Kurono Y, Nishimura M, Yanagisawa K, et al. PEN-2 enhances gamma-cleavage after presenilin heterodimer formation. *J Neurochem* 2004, 90: 1402–1413.
32. Long ZM, Zheng M, Zhao L, Xie P, Song C, Chu Y, Song W, et al. Valproic acid attenuates neuronal loss in the brain of APP/PS1 double transgenic Alzheimer’s disease mice model. *Curr Alzheimer Res* 2013, 10: 261–269.
33. Hardy J, Selkoe DJ. The amyloid hypothesis of Alzheimer’s disease: progress and problems on the road to therapeutics. *Science* 2002, 297: 353–356.
34. Flood DG, Reaume AG, Dorfman KS, Lin YG, Lang DM, Trusko SP, Savage MJ, et al. FAD mutant PS-1 gene-targeted mice: increased A $\beta$ 42 and A $\beta$  deposition without APP overproduction. *Neurobiol Aging* 2002, 23: 335–348.
35. Isoo N, Sato C, Miyashita H, Shinohara M, Takasugi N, Morohashi Y, Tsuji S, et al. A $\beta$ 42 overproduction associated with structural changes in the catalytic pore of  $\gamma$ -secretase: common effects of Pen-2 N-terminal elongation and fenofibrate. *J Biol Chem* 2007, 282: 12388–12396.
36. Siman R, Salidas S. Gamma-secretase subunit composition and distribution in the presenilin wild-type and mutant mouse brain. *Neuroscience* 2004, 129: 615–628.
37. Ni CY, Murphy MP, Golde TE, Carpenter G. gamma-Secretase cleavage and nuclear localization of ErbB-4 receptor tyrosine kinase. *Science* 2001, 294: 2179–2181.
38. Marambaud P, Shioi J, Serban G, Georgakopoulos A, Sarner S, Nagy V, Baki L, et al. A presenilin-1/gamma-secretase cleavage releases the E-cadherin intracellular domain and regulates disassembly of adherens junctions. *EMBO J* 2002, 21: 1948–1956.